Experimental investigation of double-diffusive finger convection in analog porous media: Preliminary analysis of scaling relationships for low magnitude Rayleigh space

S. E. Pringle and R. J. Glass
Flow Visualization and Processes Laboratory, Sandia National Laboratories, Albuquerque, New Mexico
sepring@sandia.gov; rjglass@sandia.gov

Introduction

Double-diffusive finger convection can occur in initially gravitationally stable, two component, miscible fluid systems when components have dissimilar molecular diffusivities and make opposing contributions to the vertical density gradients. The unequal molecular diffusivities allow for different mass transfer rates between system components which creates local buoyant instabilities. This mechanism can contribute to mass transport in porous and fractured systems leading to structured velocity fields with component fluxes that are much greater than predicted by diffusion alone (e.g. Imhoff and Green, 1988). In this paper we present results of experiments designed to investigate double-diffusive finger convection in a two component solutal system at low concentrations (< 7% by mass) within analog porous media.

Theory

The dimensionless equations that govern double-diffusive convection for a two solute system within a porous media are mass and momentum balance and advection-diffusion for each solute species:

$$\nabla^2 w = R_{S_1}\left(\nabla_{2D}{}^2 c_1 + \left(\frac{1}{R_\rho \gamma}\right)\nabla_{2D}{}^2 c_2\right), \quad \phi\frac{\partial c_1}{\partial t} - w = \nabla^2 c_1, \quad \phi\frac{\partial c_2}{\partial t} - w = \tau\nabla^2 c_2 \qquad \text{(1a-c)}$$

where the following dimensionless groups that emerge are the Rayleigh numbers for each component and the buoyancy, viscosity and diffusivity ratios:

$$R_{S_1} = \frac{\beta_1 \Delta c_1 g L k}{D_1 \nu_1}, \quad R_{S_2} = \frac{\beta_2 \Delta c_2 g L k}{D_2 \nu_2}, \quad R_\rho = \frac{\beta_1 \Delta c_1}{\beta_2 \Delta c_2}, \quad \gamma = \frac{\nu_2}{\nu_1}, \quad \tau = \frac{D_2}{D_1} \qquad \text{(2a-e)}$$

where w is the vertical velocity component, φ is the porosity, β is the volumetric expansion coefficient, c is the component concentration, g is the gravitational component acting on the fluid, L is a system lengthscale, k is the intrinsic permeability and subscript 1 and 2 represent the faster and slower diffusing component. System behavior is defined by these dimensionless groups, and when component concentrations are relatively dilute, γ and τ remain constant, and behavior for a given two solute system will be controlled by Rs_1, Rs_2 and $R\rho$.

Experimental Design

To consider convective behavior as a function of Rs_1, Rs_2 and $R\rho$, we designed a matrix of experiments using a Hele-Shaw cell. The matrix was formed by four constant buoyancy ratio transects ($R\rho$ = 1.2, 1.6, 2.0, and 2.4) in the range of Rayleigh space between 0 to 600 (Figure 1, Table 1). The initial condition was static and gravitationally stable with less dense sucrose solution over more dense salt solution in a step function configuration. Quantitative light transmission methods (e.g. Cooper et al., 1997, Detwiler et al., 1999) were used to measure concentration fields (1050x1650 points within a 15x30 cm cell) of a light absorbing dye (added to the salt solution) with high accuracy (mass conserved +/- 1%) over the course of each experiment from convective onset to full rundown (~ 400 images).

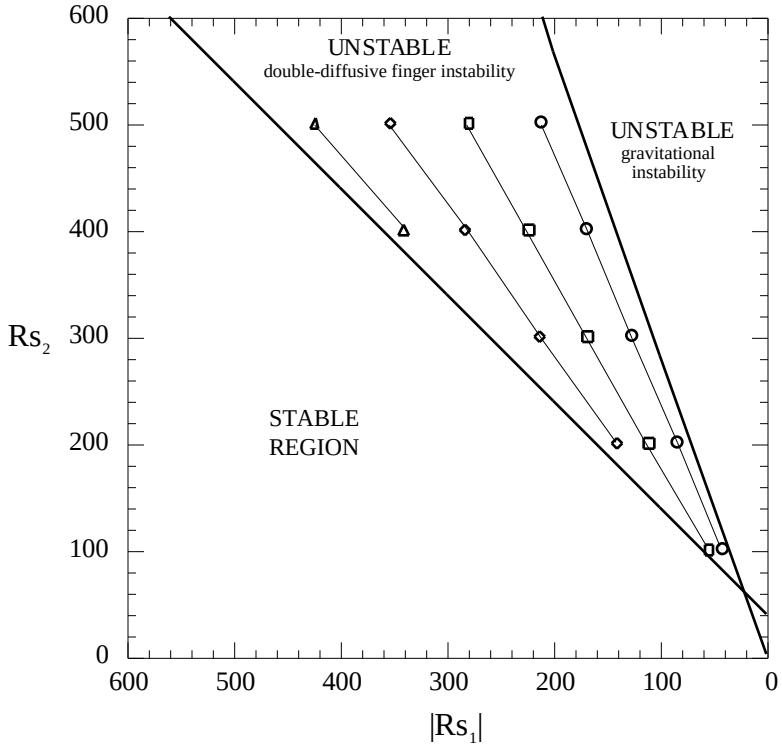

Figure 1: Rayleigh number space consisting of one stable and two unstable regions. The experimental points are shown in the double-diffusive finger instability region and were chosen to span four constant buoyancy ratio lines; 1.2 (circles), 1.6 (squares), 2.0 (diamonds), and 2.4 (triangles). Separating the stable and double-diffusive instability region is the theoretical stability boundary determined by Nield [1968] and considered experimentally by Cooper et al., [1997].

Preliminary Results

Figures 2, 3, 4, and 5 show the C/C_o field for each experiment after 10% +/- 0.04% of the initial mass of salt has crossed the midpoint of the cell (light to dark corresponds to decreasing C/C_o from 1 to 0). In general, the finger evolution along the same $R\rho$ line (moving towards the origin) results in an increase in horizontal lengthscale. The evolving fingers are relatively distinct (concentrated) and become more diffuse in appearance when moving towards the origin along a constant $R\rho$, or from lower (more unstable) to higher (more stable) $R\rho$ (i.e., downward and to the left on Figure 1). For higher Rs_i along the

$R\rho = 1.2$ line, fingers tend to move rather uniformly. As Rs_i decreases, there is more variation in the vertical position of individual fingers. For the $R\rho = 1.6$ and 2.0 experiments vertical positions of individual fingers are variable regardless of the Rs_i magnitude; however, as $R\rho$ increases to 2.4 (more stable), the fingers move uniformly. An interesting and dominating feature of the evolution for all experiments is the continual generation of small scale fingers within the region of the cell near the initial fluid-fluid interface.

Table 1: Experiments Conducted

Experiment	$R\rho$	Δc_1 kg/kg	Δc_2 kg/kg	Rs_1	Rs_2	Exp. duration (hrs)	t_c (hrs)
1	1.2	0.03463	0.05234	-212	500	16	1.017
2	1.2	0.02771	0.04167	-170	400	24	1.225
3	1.2	0.02078	0.03141	-127	300	24	1.589
4	1.2	0.01385	0.02094	-85	200	40	2.600
5	1.2	0.00693	0.01047	-42	100	47	5.650
6	1.6	0.04599	0.05234	-282	500	24	2.960
7	1.6	0.03679	0.04167	-225	400	64	3.456
8	1.6	0.02759	0.03141	-169	300	80	4.578
9	1.6	0.01840	0.02094	-113	200	95	6.583
10	1.6	0.00920	0.01047	-56	100	110	13.125
11	2.0	0.05767	0.05234	-353	500	128	8.567
12	2.0	0.04613	0.04167	-282	400	160	11.375
13	2.0	0.03460	0.03141	-212	300	180	12.969
14	2.0	0.02307	0.02094	-141	200	190	17.675
15	2.4	0.06918	0.05234	-424	500	160	26.042
16	2.4	0.05535	0.04167	-339	400	210	26.475

Subscript 1 and 2 refer to faster and slower diffusing component (salt and sucrose) and $R\rho$, Rs_1, Rs_2 are calculated based on initial conditions. The parameter t_c is the time to transfer 10% of salt mass across midpoint of cell. For all experiments: $\beta_1 = -0.755$, $\beta_2 = -0.415$, $\upsilon = 1.025\text{e-}6\ m^2s^{-1}$, $g = 9.81*\sin(25^o)$ where the angle is from the horizontal, D_1 and D_2 are 1.57e-9 and 5.53e-10 m^2s^{-1} and L (=0.0012 m) is defined as the initial thickness of the interface between the two solutions.

Table 1 lists the time to transfer 10% of salt mass across the midpoint of cell for each field shown in Figures 2-5; Figure 6 shows that for each line of constant $R\rho$, evolution time obeys a power law in Rs_1 with the exponent increasing from -1.08 for $R\rho = 1.2$ to near zero at $R\rho = 2.4$. Note, as $R\rho$ approaches τ^{-1} (2.84 for our system), the time scale will be independent of Rs_1 for a concentration range where the diffusivity remains constant.

Preliminary quantitative analysis of the data set suggests significant relations between component Rayleigh numbers, the evolution of horizontal and vertical lengthscales, and mass flux along constant buoyancy ratio lines. Results indicate a rapid progression through

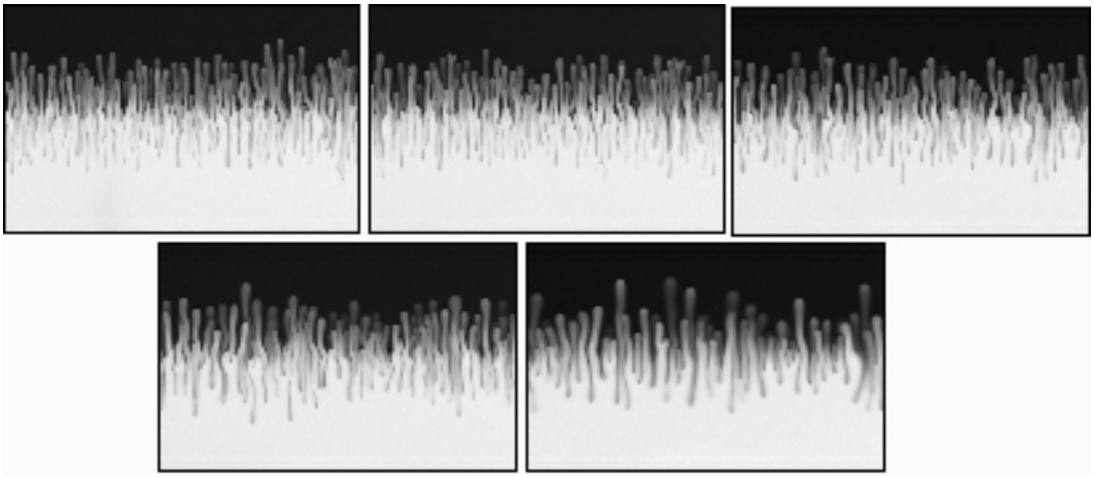

Figure 2: C/Co fields for experiments along the Rρ = 1.2 line. From left to right, top to bottom; experiment 1, 2, 3, 4 and 5 (see Table 1 for parameter definitions) after 10% of the initial mass of salt has crossed the midpoint of the cell.

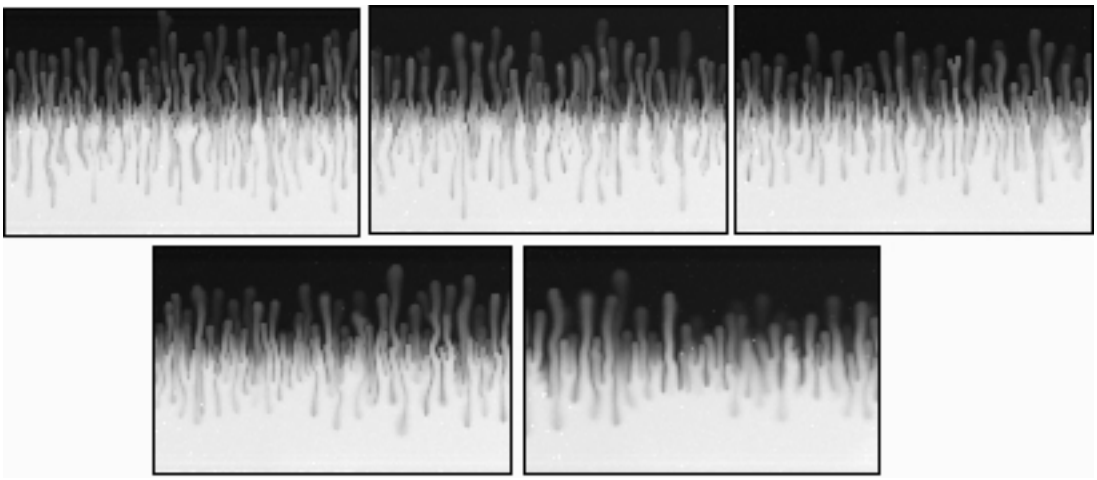

Figure 3: C/Co fields for experiments along the Rρ = 1.6 line. From left to right, top to bottom; experiment 6, 7, 8, 9 and 10 (see Table 1 for parameter definitions) after 10% of the initial mass of salt has crossed the midpoint of the cell.

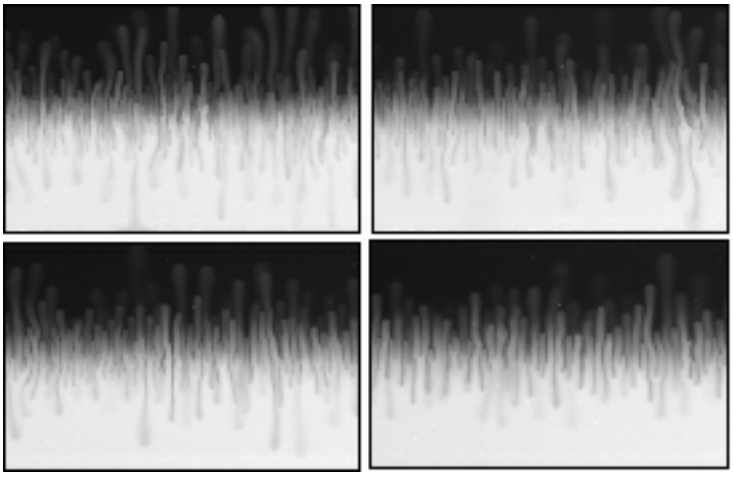

Figure 4: C/Co fields for experiments along the Rρ = 2.0 line. From left to right, top to bottom; experiment 11, 12, 13, and 14 (see Table 1 for parameter definitions) after 10% of the initial mass of salt has crossed the midpoint of the cell.

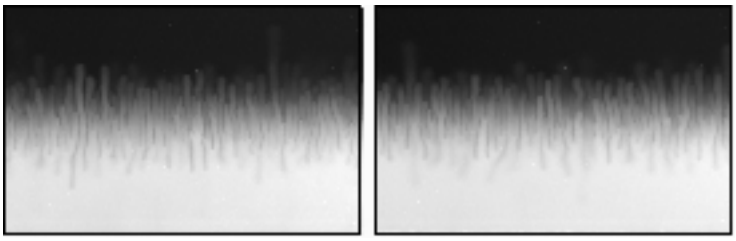

Figure 5: C/Co fields for experiments along the Rρ = 2.4 line. From left to right; experiment 15 and 16 (see Table 1 for parameter definitions) after 10% of the initial mass of salt has crossed the midpoint of the cell.

two early stages to a mature and then final rundown stage. The first stage begins at the onset of instability and shows finger development unaffected by adjacent fingers. In the second stage, fingers begin to interact and length scale evolution rates and mass fluxes are seen to decrease. This early time behavior transitions to the mature system stage where length scale evolution rates and mass fluxes again increase and follow an $R\rho$ and Rs_1 dependent behavior. Complete analysis of our data set will provide improved understanding of double-diffusive finger convection as a function of the dimensionless groups critical to system behavior.

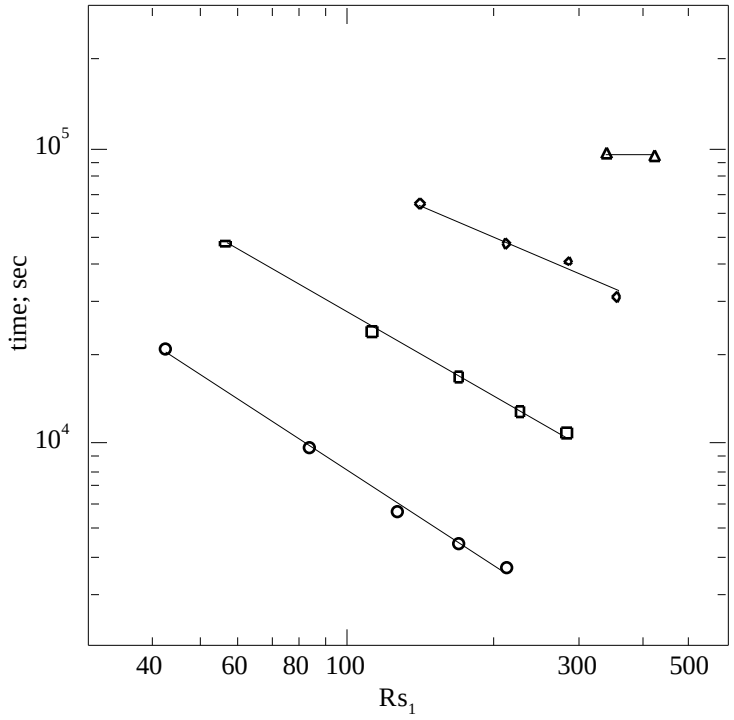

Figure 6: Relationship between time and Rayleigh number (salt component). Power law behavior gives exponent of -1.08 for $R\rho = 1.2$ line (circles), -0.93 for $R\rho = 1.6$ line (squares), -0.75 for $R\rho = 2.0$ line (diamonds), and -0.07 for $R\rho = 2.4$ line (triangles).

Acknowledgments

Financial support for this research was provided by the U.S. Department of Energy's Basic Energy Sciences Geoscience Program under contract DE-AC04-94AL85000.

References

Cooper, C.A., Glass, R.J., and S.W. Tyler, Experimental investigation of the stability boundary for double-diffusive finger convection in a Hele-Shaw cell, *Water Resour. Res*., 33, 517-526, 1997.

Detwiler, R. L., Pringle, S.E., and R.J. Glass, Measurement of fracture aperture fields using transmitted light: An evaluation of measurement error and their influence on simulations of flow and transport through a single fracture, *Water Resour. Res*., 35, 2605-2617, 1999.

Imhoff, R.T., and T. Green, Experimental investigation of double-diffusive groundwater fingers, *J. Fluid Mech.* vol 188, pp. 363-382, 1988.

Nield, D.A., Onset of Thermohaline Convection in a Porous Medium, *Water Resour. Res*., 4, 553-560, 1968.